

Characterization of DNA Adducts and Tetraols Derived from anti-Benzo[ghi]fluoranthene-3,4-dihydrodiol-5,5a-epoxide

Hui-Fang Chang,[†] Duane M. Huffer,[‡] M. Paul Chiarelli,[‡] and Bongsup P. Cho^{*,†}

Department of Biomedical Sciences, University of Rhode Island, Kingston, Rhode Island 02881 and
Department of Chemistry, Loyola University, Chicago, Illinois 60626

Received August 9, 2001

A total of seven DNA adducts and two racemic tetraols derived from anti-benzo[ghi]-fluoranthene-3,4-dihydrodiol-5,5a-epoxide (anti-B[ghi]FDE, **2**) were characterized by analyses of UV, ¹H NMR, CD, and MALDI mass spectra. The structure of **2** is the first example of a diepoxide in which a fully fused cyclopentane ring is covalently linked to the saturated ring bearing the epoxide function. Compound **2** is also a conformationally rigid structure analogue of the extensively studied anti-benzo[c]phenanthrene-3,4-dihydrodiol-1,2-epoxide (anti-BcPDE), thus serving as a model for probing the diepoxide-DNA interaction [Chang et al. (2002) *Chem. Res. Toxicol.* **15**, 198-208 (following paper in this issue)]. The most abundant adducts are formed from trans- or cis-openings of the epoxide by the amino groups of either deoxyguanosine or deoxyadenosine. Adducts of minor abundance formed by the attachment of the diepoxide to the amino group of deoxycytidine N⁴ and guanine N⁷ were also isolated. Post-source decay MALDI spectra of the (M + H)⁺ molecule ions are consistent with the assigned adduct structures. The lack of a typical benzylic proton at the site of deoxynucleoside attachment necessitated a new NMR assignment strategy. Despite the steric constraint, the epoxide ring opening of **2** occurred exclusively at the dibenzylic C5a, not at C5. The assignments on the trans- and cis-epoxide opening were made based on the molecular modeling structures, i.e., the pseudoaxial H5 in cis-adducts is placed directly under the strong influence of a shielding cone of the aromatic ring system, while the same proton in trans-adducts adopts a pseudo-equatorial conformation, thereby protruding away from the aromatic ring system. The absolute configuration at the site of deoxynucleoside attachment (C5a) was tentatively assigned on the basis of the empirical rules that have been established for deoxynucleoside-adducts derived from traditional alternant PAH diepoxides.

Introduction

Polycyclic aromatic hydrocarbons (PAHs)¹ are an important group of environmental pollutants, many of which have been implicated as a major cancer risk for humans (1, 2). Recent evidence seems to indicate that environmental and diet factors matter more than genetics in determining cancer risk (3). While the adverse effects of PAHs in humans have been recognized for many years, extensive structure–function investigations at the molecular level have been carried out only recently (4–7).

The major driving force for this was the finding that the metabolic activation of PAHs to reactive diepoxides followed by covalent binding to cellular DNA is a prerequisite for their mutagenic/carcinogenic activities (4). Another major pathway for the metabolic activation of PAHs, which has been pursued aggressively in recent years, is enzyme-catalyzed one-electron oxidation leading to radical cation intermediates that react with DNA, resulting in depurination (8). Many other mechanistic possibilities on how PAHs exert their biological outcomes have been suggested; however, the complexities of their chemistry/biology make the goal of achieving a solid structure–function relationship of PAHs difficult (9–13).

Different types of diepoxides have been implicated as the principal active metabolites of carcinogenic PAHs. Two major ones are bay- and fjord-region diepoxides, in which the oxirane ring is located in a bay- and fjord-region, respectively (4–6, 9, 14). anti- and syn-diepoxides (BaPDE, Figure 1) of benzo[a]pyrene are the most studied bay-region diepoxides. The structures of fjord- or pseudo-fjord-region diepoxides derived from benzo[c]phenanthrene (BcPDE) and 5,6-dimethylchrysene (5,6-DMCDE) differ from bay-region diepoxides in that their oxirane ring is more sterically hindered than a simple bay region (14–16). The resulting steric constraint causes the molecules to be deformed and to adopt pseudo-

* To whom correspondence should be addressed. Phone: (401) 874-5024. Fax: (401) 874-5048. E-mail, bcho@uri.edu.

[†] University of Rhode Island.

[‡] Loyola University.

¹ Abbreviations: anti-trans-tetraol, 3 α ,4 β ,5 β ,5 α -tetrahydroxy-3,4,5,5a-tetrahydrobenzo[ghi]fluoranthene; anti-cis-tetraol, 3 α ,4 β ,5 β ,5 α -tetrahydroxy-3,4,5,5a-tetrahydrobenzo[ghi]fluoranthene; BaPDE, benzo[a]pyrene-7,8-dihydrodiol-9,10-epoxide; BcPDE, benzo[c]phenanthrene-3,4-dihydrodiol-1,2-epoxide; BF-N⁷-G, 5a-(guanin-N⁷-yl)-3,4,5-trihydroxy-3,4,5,5a-tetrahydrobenzo[ghi]fluoranthene; BF-N²-dG, 5a-(deoxyguanosin-N²-yl)-3,4,5-trihydroxy-3,4,5,5a-tetrahydrobenzo[ghi]fluoranthene; BF-N⁶-dA, 5a-(deoxyadenosine-N⁶-yl)-3,4,5-trihydroxy-3,4,5,5a-tetrahydrobenzo[ghi]fluoranthene; BF-N⁴-dC, 5a-(deoxycytosine-N⁴-yl)-3,4,5-trihydroxy-3,4,5,5a-tetrahydrobenzo[ghi]fluoranthene; B[ghi]-FDE, benzo[ghi]fluoranthene-3,4-dihydrodiol-5,5a-epoxide; COSY, Correlation Spectroscopy; MALDI, matrix-assisted laser desorption ionization mass spectrometry; NOE, nuclear Overhauser effect; NOESY, nuclear Overhauser spectroscopy; PAHs, polycyclic aromatic hydrocarbons; PSD, post-source decay.

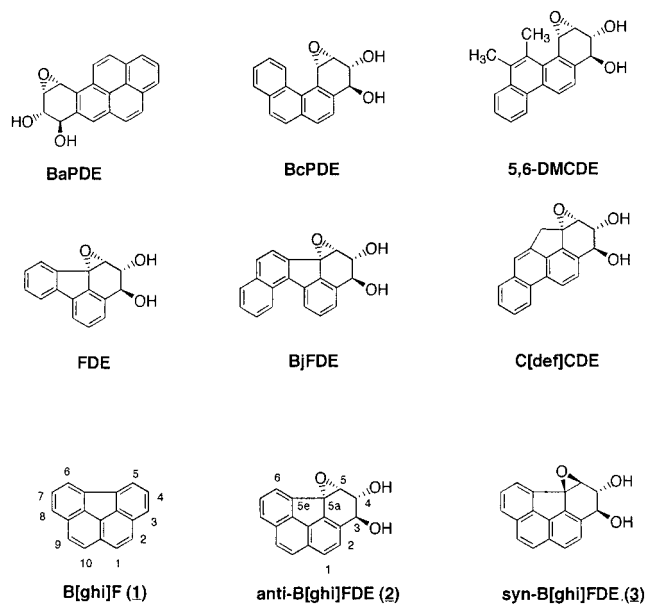


Figure 1. Examples of bay- and -fjord and highly strained pseudo-fjord-region diolepoxides, benzo[a]pyrene-7,8-dihydrodiol-9,10-epoxide (BaPDE), benzo[c]phenanthrene-11,12-dihydrodiol-13,14-epoxide (BcPDE), 5,6-dimethylchrysene-1,2-dihydrodiol-3,4-epoxide (5,6-DMCDE), fluoranthene-2,3-dihydrodiol-1,10b-epoxide (FDE), benzo[j]fluoranthene-4,5-dihydrodiol-6,6a-epoxide (BjFDE), and cyclopenta[def]chrysene-1,2-dihydrodiol-3,3a-epoxide (C[def]CDE); the structures of benzo[ghi]fluoranthene (B[ghi]F, **1**) and its anti- and syn-diolepoxides, anti- and syn-3,4-dihydrodiol-5,5a-epoxides (B[ghi]FDE, **2** and **3**).

diequatorial diol conformations. Such unusual diolepoxide structures are related to the high reactivity with DNA and a preferential affinity to dA over dG, which may be responsible for their exceptionally high mutagenicity/tumorigenicity (5, 14–19). A group of “highly strained” and “nonclassical” diolepoxides studied recently include fluoranthene-2,3-dihydrodiol-1,10b-epoxide (FDE) (20), benzo[j]fluoranthene-4,5-dihydrodiol-6,6a-epoxide (BjFDE) (21), and cyclopenta[def]chrysene-1,2-dihydrodiol-3,3a-epoxide (C[def]CDE) (Figure 1) (22). The structures of FDE and BjFDE are unique in that a trisubstituted epoxide ring is fused with a five-membered ring. C[def]CDE shares a similar trisubstituted epoxide ring, but a methylene bridge is part of the fused ring system. These diolepoxides were shown to be considerably tumorigenic although they are less active than anti-BcPDE and anti-BaPDE (23, 24).

Benzo[ghi]fluoranthene (**1**, Figure 1) is an environmental pollutant commonly found in coal tar (25), carbon black (26), tobacco and marijuana smoke (27), and many foods but is found to be inactive as a complete carcinogen on mouse skin (28). The *in vivo* metabolic fates of **1** have not been established. The structure of **1** is unique in that the four sides of the fjord-region are completely fused with a benzo[c]phenanthrene ring system. The crystal structure suggests that **1** is planar with the bonds in the cyclopentane ring that are longer than those in a typical fused six-membered ring system having a Kékulé structure (29). We have recently prepared anti- and syn-benzo[ghi]fluoranthene 3,4-dihydrodiol-5,5a-epoxides (anti- and syn-B[ghi]FDE, **2** and **3**, Figure 1) as putative diolepoxide metabolites of **1** (30). The structures of **2** and **3** represent a new type of diolepoxides in which a fully fused cyclopentane ring is covalently linked to the saturated ring bearing an epoxide function. Similar to other highly

strained diolepoxides (20–22), **2** and **3** are also found to be relatively stable. Due to their unique molecular rigidity and their structural similarity to BcPDE (Figure 1), **2** and **3** could serve as model systems for probing the specific roles of molecular deformity and diol conformation in the interaction of diolepoxides with DNA. The following paper in this issue reports comparative DNA binding studies involving reactions of **2**, **3**, and anti-BcPDE. In this report, we describe spectral characterization of DNA-adducts and tetraols derived from *in vitro* reactions of the racemic **2** with calf-thymus DNA.

Experimental Procedures

Chemicals. Caution: anti-B[ghi]FDE should be regarded as a potential carcinogen and any skin contact should be avoided. Racemic anti-B[ghi]FDE (**2**) was prepared as described previously (30). Poly(dG-dC)·poly(dG-dC) and poly(dA-dT)·poly(dA-dT), calf-thymus DNA, DNase I, snake venom phosphodiesterase, and alkaline monophosphatase were all purchased from Sigma (St. Louis, MO). Reagent- and HPLC-grade solvents were obtained from Fisher (Pittsburgh, PA). All other chemicals were purchased from Aldrich (Milwaukee, WI).

Reaction of **2 with Calf-Thymus DNA.** A racemic mixture of **2** in 8 mL of acetone (1 mg/mL) was added to 20 mL of Tris-HCl buffer (50 mM, pH 7.0) containing calf-thymus DNA (1 mg/mL). The mixture was incubated under dark at 37 °C for 24 h. The reaction mixture was extracted with ethyl acetate (3 × 40 mL) and then with ethyl ether (2 × 40 mL) to remove unreacted diolepoxide and hydrolyzed tetraols. Traces of the remaining organic solvents in the aqueous solution were evaporated with the aid of a stream of N₂. The resulting DNA solution, which was restored to the original volume by adding water, was enzymatically digested to deoxynucleosides using a general three-step procedure (34). To the DNA solution was added a mixture of 0.5 mL of 1 M magnesium chloride, 1 mL of 1% sodium azide and 10 000 kilounits of DNase I (5.6 mg) in 1.3 mL of 50 mM Tris-HCl buffer (pH 7.0). After incubating the mixture overnight at 37 °C, 1.5 mL of 1.0 M Tris base and 1.6 units of snake venom phosphodiesterase in 1.3 mL of 0.2 M Tris-HCl buffer (pH 9.0) were added, and the digestion was continued at 37 °C in the dark for 46 h. The mixture was then treated with 100 units of alkaline monophosphatase and the digestion continued at 37 °C under dark overnight. A Waters C18 Sep-Pak (Milford, MA) was preconditioned with 20 mL of methanol and 20 mL of water before use. The digested DNA solution was diluted with 40 mL of 0.2 M phosphate buffer (pH 7.0), and then deposited onto the Sep-Pak. It was eluted first with 50 mL of water, followed by six 5-mL vol of methanol. The methanol fractions containing the adducts were combined, evaporated to dryness, and separated using HPLC.

Reaction of **2 with poly(dG-dC)·poly(dG-dC) and poly(dA-dT)·poly(dA-dT).** An aliquot of a poly(dG-dC)·poly(dG-dC) solution (1.3 mL, 1 mg/mL) in Tris-HCl buffer (50 mM, pH 7.0) was combined with a solution of **2** in acetone (1 mL, 1 mg/mL). The mixture was incubated at 37 °C in dark for 20 h and worked-up as described above for reaction with calf-thymus DNA. After an ether extraction to remove tetraols and the unreacted diolepoxide, the aqueous solution was successively digested with 30 μL of 1 M magnesium chloride, 50 μL of 1% sodium azide, 625 kilounits of DNase I (0.35 mg) in 80 μL of 50 mM pH 7.0 Tris-HCl buffer, 100 μL of 1 M Tris base, 0.1 units of snake venom phosphodiesterase in 80 μL of 0.2 M Tris-HCl Buffer (pH 9.0), and 6.25 units of alkaline monophosphatase. Methanol fractions from a Sep-Pak extraction were analyzed on a reverse phase HPLC. A reaction with poly(dA-dT)·poly(dA-dT) was conducted similarly as described above with poly(dG-dC)·(dG-dC).

Chromatography and Instrumentation. HPLC separations were conducted on a Waters Associate HPLC system equipped with model 501 pumps, a U6K injector, a 680

automated gradient controller, and a Hitachi L-3000 photodiode array detector. Analytical separation of adducts and tetraols was conducted by using the following columns with 50–70% methanol in water as a mobile phase at a flow rate of 1.0 mL/min: Ultrasphere ODS (4.6 mm × 25 cm, 5 μm, Beckman), Vydac ODS (4.6 mm × 25 cm, 5 μm, Vydac), and Partisil ODS2 (4.6 mm × 25 cm, 5 μm, Whatman). For semipreparative scale separation, a Beckman semi-prep Ultrasphere ODS column (10 mm × 25 cm, 5 μm) with a flow rate of 2.0 mL/min was used. Specific HPLC conditions are indicated in the text and the figure legends. Combined HPLC samples were concentrated using a model AES1000-120 SpeedVac concentrator (Forma Scientific, Inc., Marietta, OH). UV spectra were recorded on a Hitachi U-2000 UV–Vis spectrophotometer. CD spectral measurements were made in methanol on a Jasco model J500A spectropolarimeter (National Center for Toxicological Research, Jefferson, AR). Molecular modeling work was conducted using version 3.0 version of the CAChe default MM2 force field.

NMR. ¹H NMR spectra were recorded at ambient temperature on a Bruker AM300 NMR spectrometer, operating at 300 MHz. Chemical shifts were expressed in ppm with respect to TMS by assigning the tallest residual solvent peak; 2.05 and 3.31 ppm for acetone-*d*₆ and methanol-*d*₄, respectively. COSY, NOESY, one-dimensional NOE difference, and decoupling experiments were conducted using standard Bruker software.

Mass Spectrometry. Matrix-assisted laser desorption ionization (MALDI) mass spectra of adducts and tetraols were acquired with an R. M. Jordan, Co. (model D850) time-of-flight mass spectrometer (Grass Valley, CA). A nitrogen laser was used to induce desorption and ionization. α-Cyano-4-hydroxycinnamic acid and 2,6-dihydroxyacetophenone were used as matrixes for adducts and tetraols, respectively, as described previously (31, 32). The deoxynucleoside adducts formed protonated fragment ions by cleavage of the glycosidic bond, as well as protonated molecule ions (M + H)⁺ and molecule ions formed by the attachment of a sodium ion, (M + Na)⁺. No protonated or sodiated molecule ions were observed when tetraols and matrix were analyzed alone, so the matrix analyte solutions were mixed with 0.025 M LiNO₃ for the purpose of generating (M + Li)⁺ molecule ions. PSD product ion spectra were acquired with a PerSeptive Biosystems, Inc. Voyager DE-RP mass spectrometer (Framingham, MA) at the Washington University Resource for Biomedical and Bio-organic Mass Spectrometry in St. Louis, MO. The instrument was operated in the continuous ion extraction mode with a total acceleration potential of 25 kV. The background signal level was determined by analyzing the matrix mixture alone in the same mass window(s) in which the molecule ions were selected for PSD analysis. Normally, 20–30 laser shots were averaged to produce a PSD spectrum. The instrument and procedures are described in more detail elsewhere (33).

Results

Isolation of Tetraols and DNA Adducts. After the reaction, the tetraols and the unreacted diepoxide were extracted with ether, while modified DNA adducts in the aqueous layer were further subjected to a three-step enzymatic digestion process (DNase/phosphodiesterase/alkaline phosphatase) that transformed them into deoxynucleosides. Sufficient amounts of tetraols and deoxynucleoside adducts were isolated and purified by HPLC for spectral characterization.

Figure 2a shows the HPLC profile of an enzyme-hydrolysate derived from *in vitro* reactions of the racemic **2** with calf-thymus DNA. In addition to highly polar natural deoxynucleosides (marked as X) and tetraol (T), the hydrolysate contains at least seven deoxynucleoside adducts, which are labeled as anti-1–7 according to their order of elution. Compound **2** was reacted with poly(dG-dC)·poly(dG-dC) and poly(dA-dT)·(dA-dT) individually

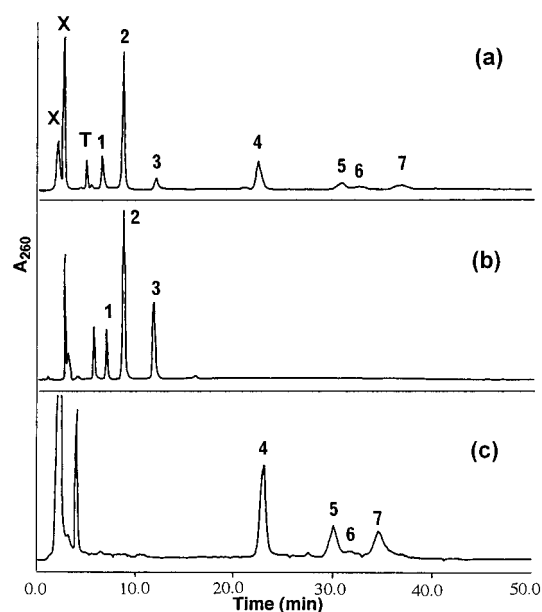


Figure 2. HPLC chromatograms obtained from the reaction of the racemic anti-B[ghi]FDE (**2**) with (a) calf-thymus DNA; (b) poly(dG-dC)·poly(dG-dC); and (c) poly(dA-dT)·poly(dA-dT). The adducts are numerically labeled by decreasing order of polarity: anti-trans-BF(S)-N⁷-G (anti-1), anti-trans-BF(R,S)-N²-dG (anti-2), anti-trans-BF(S)-N⁴-dC (anti-3), anti-trans-BF(R)-N⁶-dA (anti-4), anti-trans-BF(S)-N⁶-dA (anti-5), anti-cis-BF(R)-N⁶-dA (anti-6), anti-cis-BF(S)-N⁶-dA (anti-7) (see Figure 3 for the structures); X, nonmodified deoxynucleosides; T, tetraols (Vydac ODS, 4.6 × 25 mm, 5 μm, 50% methanol/water, 1 mL/min).

and the results are summarized Figure 2. It is clear from comparison that anti-1, 2, and 3 are derived from dG (or dC), while the more lipophilic fractions anti-4, 5, 6, 7 are from dA (or dT). Consistent with this classification, the earlier eluting anti-1,2,3 adducts showed poor solubility in acetone as compared to the latter eluting adducts (anti-4,5,6,7). Figure 3 shows the full structures of tetraols and deoxynucleoside adducts obtained from the opening of the epoxide ring of each enantiomer of **2** at the dibenzyllic position (i.e., C5a) by the exocyclic amino groups of either dG (N²) or dA (N⁶) or dC (N⁴) residues via either trans or cis opening. Also included in Figure 3 is the structure of a minor guanine-N⁷ adduct, which is derived from the epoxide opening by the N⁷ guanine, followed by a cleavage of the sugar moiety. The absolute configuration assignment (R or S) at C5a in Figure 3 is tentative (see below).

With native calf-thymus DNA, 57% of **2** was converted into DNA adducts. The relative percentage amount of adducts is as follows, assuming their extinction coefficients are similar at 260 nm: anti-1 (9.7%), anti-2 (44.8%), anti-3 (2.5%), anti-4 (26.5%), anti-5 (11.1%), anti-6 (1.1%), and anti-7 (4.3%).

Structure Characterization. A total of seven adducts and two racemic tetraols have been isolated: anti-trans-BF(S)-N⁷-G (anti-1), anti-trans-BF(R or S)-N²-dG (anti-2); anti-trans-BF(S)-N⁴-dC (anti-3), anti-trans-BF(R)-N⁶-dA (anti-4), anti-trans-BF(S)-N⁶-dA (anti-5), anti-cis-BF(R)-N⁶-dA (anti-6), anti-cis-BF(S)-N⁶-dA (anti-7), anti-trans-tetraol, anti-cis-tetraol (Figure 3). The structures of these adducts and tetraols isolated by HPLC were determined using a variety of spectroscopic techniques. The rationale associated with the spectral interpretation used to arrive at the structures of these compounds was similar in each case. The elucidation of

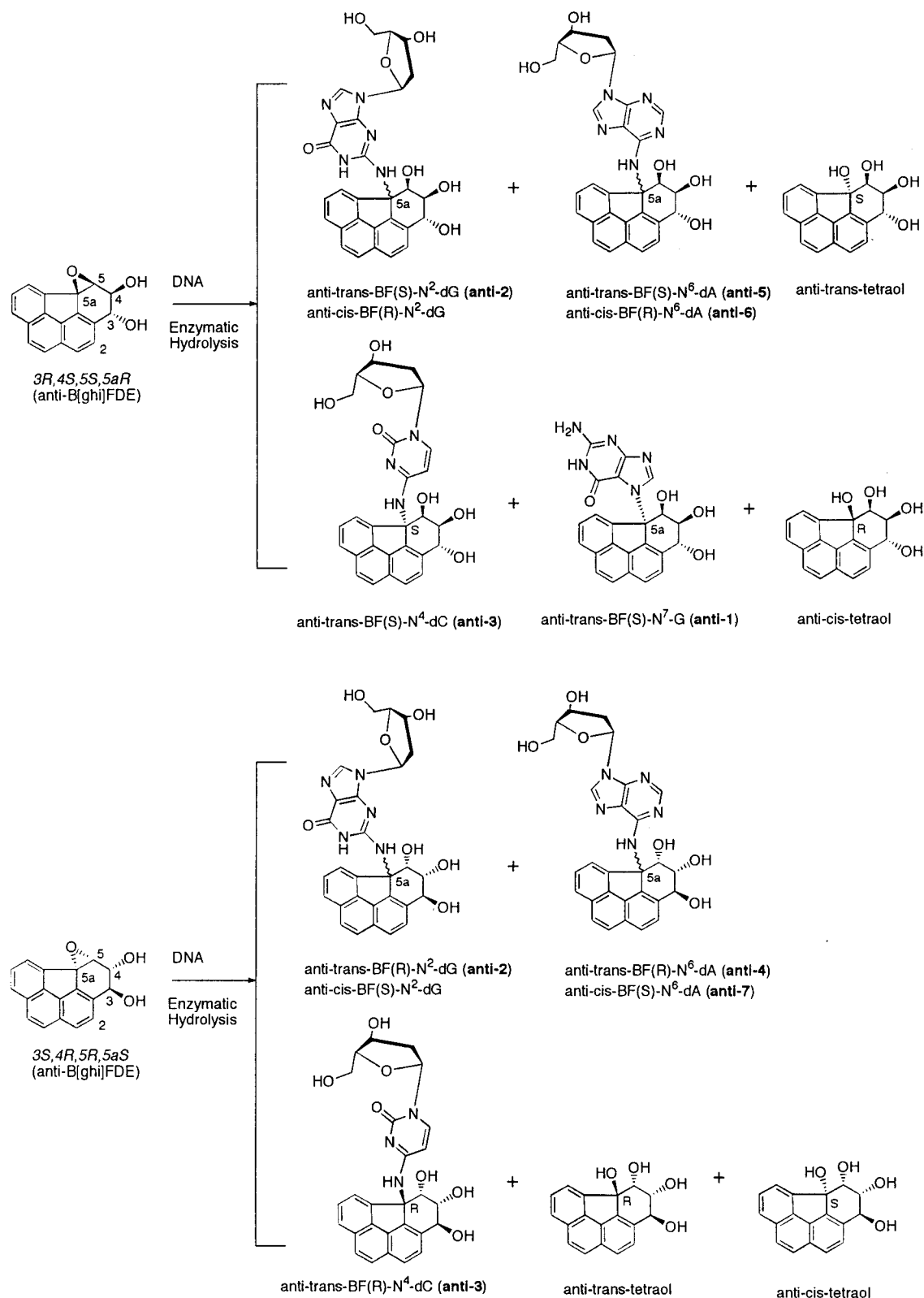


Figure 3. Structures of DNA adducts and tetraols derived from reaction of the racemic anti-B[ghi]FDE (**2**). The adducts that were isolated are labeled as anti-1–7 according to the numbering in the HPLC profile given in Figure 2. The absolute configuration assignment (S or R) at the deoxynucleoside attachment (C5a) is specified. anti refers to a relative epoxide/benzylic hydroxyl configuration of **2**, i.e., the epoxide oxygen is on the opposite side of the molecule relative to the benzylic hydroxyl group. trans and cis refer to the reaction pattern of epoxide ring opening, where it occurs from the opposite or same side, respectively.

the structures of the B[ghi]-dA adduct pair, anti-4 and -5, are presented in detail as illustrative examples.

anti-trans-BF(R)-N⁶-dA (anti-4); *anti-trans-BF(S)-N⁶-dA* (anti-5). The ¹H NMR (Table 1) and MALDI mass

spectral (Table 2) data of anti-4 are consistent with the B[ghi]F-dA adduct structure. Figure 4 is a MALDI-PSD product ion spectrum of the protonated molecule ion of B[ghi]F-dA at *m/z* 528. The most prominent fragmenta-

Table 1. ¹H NMR Data for Adducts and of Tetraols Derived from anti-B[ghi]FDE (2)^a

compd	N-H	methine hydrogens (ppm)			<i>J</i> _{3,4} , <i>J</i> _{4,5} (Hz)		aromatic protons
		H ₃	H ₄	H ₅			
anti-B[ghi]FDE (2)		5.12	3.95	4.53	8.1, 1.2	7.6–8.0 (H _{1,2,6–10})	
anti-trans-tetraol		4.65	4.88	4.80	7.1, 2.2	7.8–7.7 (H _{1,8,9,10}), 7.47 (H ₇ , <i>J</i> _{7,8} = 8.0 Hz), 7.56 (H ₂ , <i>J</i> _{1,2} = 8.3 Hz), 7.64 (H ₆ , <i>J</i> _{6,7} = 7.1 Hz)	
anti-cis-tetraol		5.28	4.28	3.78	1.7, 3.6	7.75–7.85 (H _{1,3,4,5,6,8}), 7.58 (H ₂ , <i>J</i> _{1,2} = 8.3 Hz), 7.52 (H ₇ , <i>J</i> = 7.6 Hz)	
anti-trans-BF(S)-N ⁷ -G (anti-1) ^b		4.65	4.36	5.62	7.1, 6.6	8.1–7.5 (H _{1,2,6–10}), 7.25 (bs, Gua-H ₈)	
anti-trans-BF(R,S)-N ² -dG (anti-2)	7.23 (br)	4.73	4.78	5.97	6.9, 2.1	8.29 (H ₆ , <i>J</i> _{6,7} = 7.1 Hz), 7.84 (H ₁ , <i>J</i> _{1,2} = 8.3 Hz), 7.79 (H _{9,10}), 7.75 (H ₈ , <i>J</i> _{7,8} = 8.0 Hz), 7.62 (H ₂), 7.45 (H ₇), 8.07 (bs, Gua-H ₈)	
anti-trans-BF(R)-N ⁴ -dC (anti-3) ^b	ND	4.70	4.62	6.01	7.0, 2.0	8.40 (H ₆ , <i>J</i> _{6,7} = 7.1 Hz), 7.80 (H ₁ , <i>J</i> _{1,2} = 8.3 Hz), 7.75 (H _{9,10}), 7.70 (H ₈ , <i>J</i> _{7,8} = 8.2 Hz), 7.59 (H ₂), 7.45 (H ₇) 7.87 (Cyt-H ₆), 5.86 (Cyt-H ₅ , <i>J</i> _{5,6} = 7.53 Hz)	
anti-trans-BF(R)-N ⁶ -dA (anti-4)	7.12 (bs)	4.71	4.76	6.04	6.7, 1.9	8.30 (H ₆ , <i>J</i> _{6,7} = 7.8 Hz), 7.84 (H ₁ , <i>J</i> _{1,2} = 8.3 Hz), 7.77 (H _{9,10}), 7.71 (H ₈ , <i>J</i> _{7,8} = 8.2 Hz), 7.64 (H ₂ , <i>J</i> _{1,2} = 8.3 Hz), 7.41 (H ₇), 8.50 (Ade-H ₂), 8.21 (Ade-H ₈)	
anti-trans-BF(S)-N ⁶ -dA (anti-5)	7.10 (bs)	4.72	4.76	6.06	7.1, 2.0	8.33 (H ₆ , <i>J</i> _{6,7} = 7.8 Hz), 7.84 (H ₁ , <i>J</i> _{1,2} = 8.3 Hz), 7.76 (AB, H _{9,10}), 7.72 (H ₈ , <i>J</i> _{7,8} = 8.3 Hz), 7.63 (H ₂ , <i>J</i> _{1,2} = 8.3 Hz), 7.41 (H ₇), 8.52 (Ade-H ₂), 8.22 (Ade-H ₈)	
anti-cis-BF(R)-N ⁶ -dA (anti-6) ^b	ND	5.48	4.06	3.12	4.2, 6.7	7.62–7.91 (H _{1,2,6,8,9,10}), 7.50 (H ₇), 7.82 (Ade-H ₂), 8.31 (Ade-H ₈)	

^a Spectra were measured in acetone-*d*₆ with D₂O except where indicated. Chemical shifts are reported in ppm and coupling constants are given in hertz (Hz). bs (broad singlet); ND, not detected. The spectrum of anti-7 is not included due to low signal-to-noise ratio, but overall spectral shape is essentially identical to that of anti-6. ^b Taken in methanol-*d*₄. See Figures 1 and 3 for full structures.

Table 2. Time-of-Flight MALDI Mass Spectra Data for Adducts and of Tetraols Derived from anti-B[ghi]FDE (2)

compd	mass ions (relative abundance)			
	[M - dR] ⁺	[M + H] ⁺	[M + Li] ⁺	[M + Na] ⁺
anti-trans-tetraol			301(100)	
anti-cis-tetraol			301(100)	
anti-trans-BF(S)-N ⁷ -dG (anti-1)		428 (100)		
anti-trans-BF(R,S)-N ⁶ -dG (anti-2)	428 (100)	544 (45)		566 (85)
anti-trans-BF(R)-N ⁴ -dC (anti-3)	388 (40)	504 (100)		
anti-trans-BF(R)-N ⁶ -dA (anti-4)	412 (50)	528 (100)		
anti-trans-BF(S)-N ⁶ -dA (anti-5)	412 (50)	528 (100)		
anti-cis-BF(R)-N ⁶ -dA (anti-6)	412 (70)	528 (100)		
anti-cis-BF(S)-N ⁶ -dA (anti-7)	412 (50)	528 (100)		

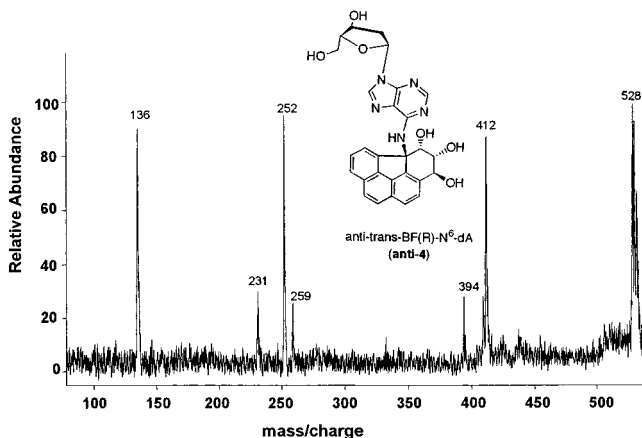


Figure 4. MALDI-PSD product ion mass spectrum of the protonated molecule ion (M + H)⁺ at *m/z* 528 from the B[ghi]F-(R)dA adduct (anti-4).

tion ion is the protonated base at *m/z* 412, formed by the loss of the 2'-deoxyribose. Other abundant ions in this spectrum are the protonated dA (*m/z* 252) and adenine base (*m/z* 136). Product ions formed by successive losses of H₂O and CO from the benzo[ghi]fluoranthene fragment (R - H₂O, *m/z* 259 and R - H₂O - CO, *m/z* 231) are much less abundant. The relative abundances of the most

significant source-produced ions in the molecular weight analysis of other adducts and tetraols are summarized in Table 2.

Figure 5 shows an expanded region of the ¹H NMR spectra recorded in acetone-*d*₆ with and without addition of D₂O. The chemical shifts of the major signals and coupling constants are summarized in Table 1. The spectrum showed nine well-resolved aromatic protons, except for the fluoranthenes H₉ and H₁₀, which appeared as an AB quartet centered at 7.77 ppm. The two sharp signals at 8.21 and 8.50 ppm, which were not observed prior to reaction, have been assigned to the adenine H₈ and H₂ protons, respectively. Consistent with this, irradiation of the sharp 8.21 ppm singlet gave an NOE to the anomeric H_{1'} sugar proton. The D₂O exchangeable broad singlet at 7.12 ppm was assigned to the N-H proton at the site of dA attachment. The presence of a 2'-deoxyribose sugar moiety in the molecule is evidenced by the observation of a series of the sugar and exchangeable protons in the 2.0–6.5 ppm range, all of which have been accounted for through analyses of COSY and decoupling experiments. The remaining signals in the region should belong to the fluoranthene H_{3,4,5} methine proton network. The clean doublet of doublets signal centered at 4.76 ppm was readily recognized as H₄ based on its simultaneous couplings to H₃ and H₅. The upfield

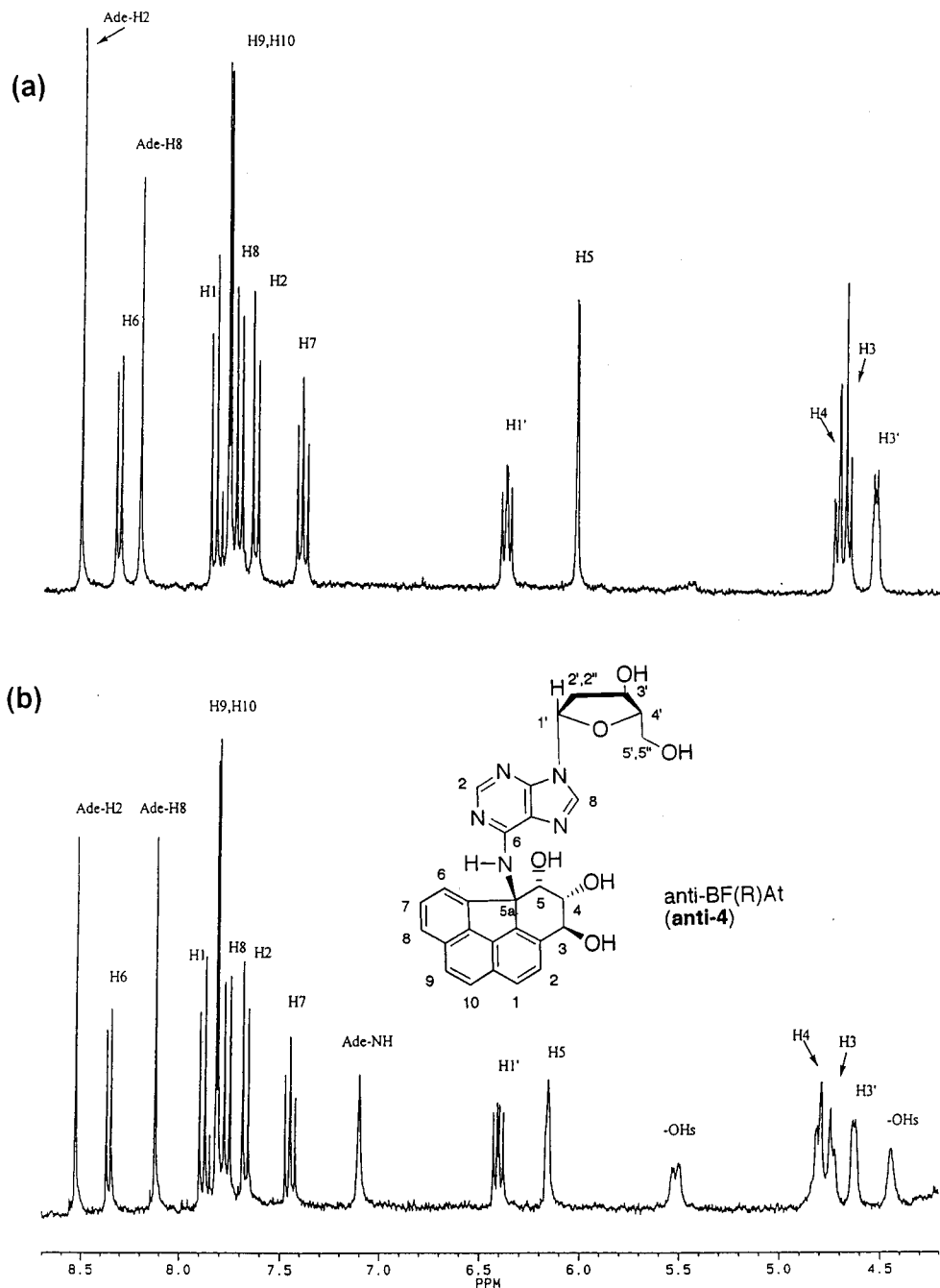


Figure 5. Partial ^1H NMR spectrum of anti-4 recorded in acetone- d_6 (a) with or (b) without the addition of D_2O . The adenine-H2 and H8 appears at 8.50 and 8.21 ppm, respectively. Protons designated with a prime symbol are derived from the 2'-deoxyribose sugar. NOEs are observed for H2–H3, H5–H6, H8–H1', H4–H5, and H3–H4.

doublet at 4.71 ppm showed an NOE to the highly shielded, peri aromatic H2 at 7.64 ppm and was thus assigned to H3 ($J_{3,4} = 6.7$ Hz). The remaining clean doublet at 6.04 ppm with a small coupling ($J_{4,5} = 1.9$ Hz) must be H5. Additional NOE experiments were conducted to further support the structure assignment and the results are summarized in the legend of Figure 5.

(i) *Site of Purine Substitution.* Analysis of the NMR data indicated that the epoxide ring opening occurred at the sterically hindered dibenzylic C5a, not at C5. First, H5 is significantly deshielded (-1.24 to 1.51 ppm) compared to anti-trans-tetraol (below) and **2** (Table 1). If the opening had occurred at C5, H5 should have experienced a significant shielding (5). Second, the appearance of the exchangeable N–H proton at 7.12 ppm

as a clean singlet signal indicates the absence of a vicinal proton at the site (C5a) of dA attachment. In general, a relatively large coupling (6–14 Hz) with the adjacent benzylic proton has been observed for the N–H proton of traditional deoxynucleoside adducts (such as BPDE or BcPDE) (5). Third, a significant deshielding (-0.8 ppm) of the fluoranthene H6, going from anti-tetraol to anti-4, may be due to its close spatial proximity of the purine ring in the adduct molecule. Finally, irradiation of H6 resulted in an NOE enhancement on both N–H and H5, indicating their close spatial proximity. The distance between H5 and H6 was calculated to be about 3.1 Å. Taken all together, it was concluded that the epoxide ring opening of **2** occurred in the expected manner to allow reaction at the dibenzylic site, C5a.

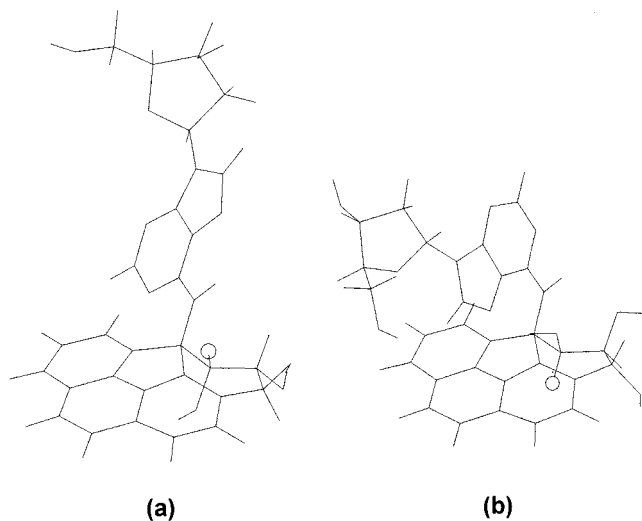


Figure 6. Energy-minimized structures for the deoxynucleoside adducts formed upon (a) trans (anti-4)- and (b) cis (anti-6)-attack at C5a by the amino group of dA. Note the location of the pseudoaxial H5 (represented by a small circle) of anti-6 is located directly under the influence of a shielding cone, whereas the same proton of the trans-opened anti-4 adduct adopts pseudoequatorial, which protrudes away from the PAH ring system.

(ii) *Stereochemistry of Addition.* The lack of a typical benzylic proton at the site (C5a) of deoxynucleoside attachment in the B[ghi]F-deoxynucleoside adducts prevented us from using the general ^1H NMR procedure that has been successfully used for assigning the stereochemistry of addition of adducts derived from conventional diolepoxides (5). Molecular modeling analysis, however, indicated that a conformational distinction exists between the cis- and trans-B[ghi]F-deoxynucleoside adducts. Figure 6 shows the energy minimized structures of anti-4 and anti-6 as a representative example of trans- and cis-epoxide opening adducts, respectively. Due to the rigidity of **2**, the incoming deoxynucleoside must occupy a pseudoaxial position at C5a for both trans- and cis-adducts. As a result, H5 in the trans-adduct (anti-4, Figure 6a) adopts a pseudoequatorial conformation (shown in a small circle) and protrudes away from the PAH ring system. On the other hand, the same proton in the cis-adduct (anti-6, Figure 6b) will be placed directly under the influence of a shielding cone of the aromatic ring moiety. It was found that the H5 resonances of anti-4 and -5 were deshielded significantly (~ 2.9 ppm) relative to those of anti-6 and -7. Therefore, the anti-4 and -5 and anti-6 and -7 diastereomeric pairs were assigned to the trans- and cis-opening adducts, respectively. A relatively small change in the $J_{3,4}$ and $J_{4,5}$ coupling constants going from anti-trans-tetraol ($J_{3,4} = 7.1$ and $J_{4,5} = 2.2$ Hz) to the adduct ($J_{3,4} = 6.9$ and $J_{4,5} = 2.0$ Hz) also suggested minimal conformational change during such a transition. The observed small $J_{4,5}$ coupling constant does not seem to correlate with the calculated H4-C4-C5-H5 dihedral angle value (55°). A better correlation, however, exists for the adducts derived from syn-B[ghi]FDE (following paper in this issue).

Anti-4 and -5 gave essentially the same UV, MALDI-mass, and ^1H NMR spectra. However, their CD spectra are a mirror image of each other (Figure 8a), indicating that the structure of anti-5 is identical to anti-4, differing only in the configuration at C5a where dA is attached. The majority of ^1H NMR and MALDI-fragmentation

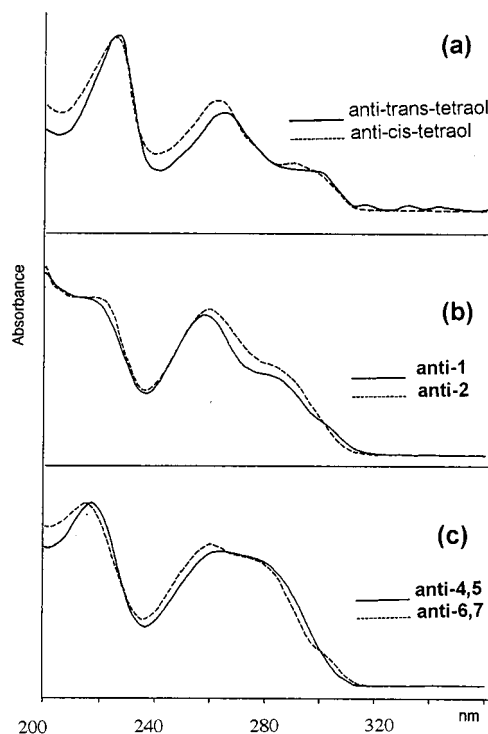


Figure 7. The normalized on-line UV spectra of (a) tetraols; (b) anti-BF(S)-N⁷-G (anti-1) (—) and anti-BF-N²-dG (anti-2) (---); and (c) anti-BF-N⁶-dA adducts derived by trans (—) and cis (---) opening of **2**. The spectra of the diastereomeric pair (i.e., anti-4 and -5, and anti-6 and -7) at the site of deoxynucleoside attachment (C5a) are essentially identical.

signals have been assigned and summarized in Tables 1 and 2, respectively. Assignment of absolute configuration at C5a was not possible since the racemic mixture of **2** was used in the present study. Nevertheless, tentative assignments were made on the basis of the empirical correlation rules that have been used for adducts derived from conventional diolepoxides. It has been shown that the sign of the most intense CD band in the 250–280 nm region is positive if the absolute configuration at the N-substituted benzylic carbon of the aromatic moiety is “S” and negative when the configuration is “R” (5). Accordingly, the absolute configuration at C5a of anti-adducts 4 and 5 were tentatively assigned as R and S, respectively (Figure 8a).

anti-cis-BF(R)-N⁶-dA (anti-6); anti-cis-BF(S)-N⁶-dA (anti-7). The MALDI-PSD product ion spectra of anti-6 and -7 are virtually identical to those of the dA adduct pair (anti-4 and -5) described above (Table 2). The UV spectra of anti-6 and -7 are also identical, but their absorption maxima in methanol is slightly shifted to a shorter wavelength and shows a better defined shoulder at 275 nm relative to those of the trans-opened dA adducts (anti-4 and -5) (Figure 7c). The CD spectra of anti-6 and anti-7 are essentially mirror images of one another, but are clearly distinguishable from those of anti-4 and -5 (Figure 8b). Since anti-4 and -5 have already been assigned to the diastereomeric pair of the anti-trans-dA adducts, anti-6 and -7 must be the diastereomeric dA adduct pair at C5a with the cis epoxide opening.

The major ^1H NMR signals of anti-6 have been assigned in the same manner as described above for anti-4 and anti-5. The chemical shift and coupling patterns of the H3,4,5 methine protons closely resemble those of anti-cis-tetraol (Table 1). In particular, the relatively large

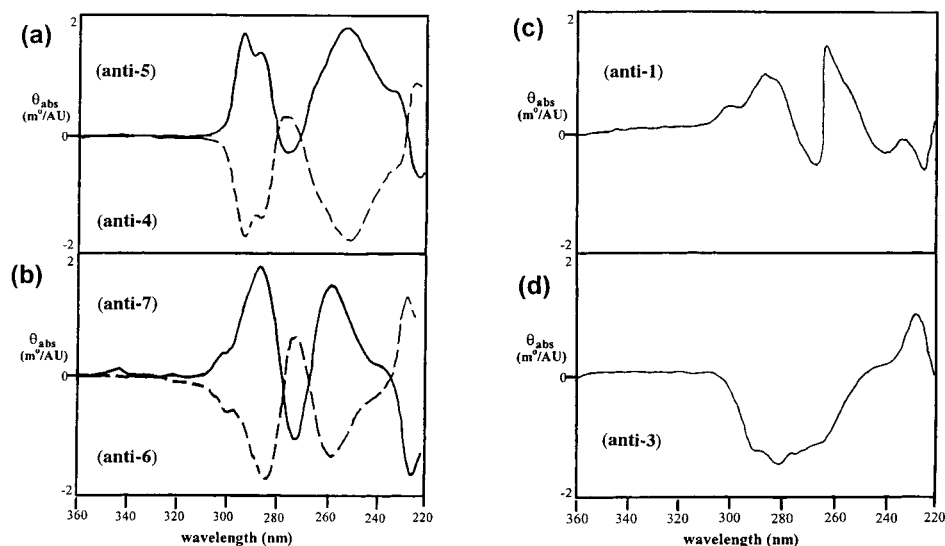


Figure 8. CD spectra of the adducts derived from (a) the trans (anti-4 and -5)- and (b) cis (anti-6 and -7)-openings at C5a by the amino group of dA; trans-opening by (c) the N⁷ of guanine (anti-1) and (d) the exocyclic amino group of dC (anti-3). The spectra were taken in pure methanol and are labeled according to the numbering in Figure 2. See Figure 3 for the chemical structures.

$J_{4,5}$ coupling constant (6.7 Hz) and a strong shielding of H5 (3.12 ppm) (see above) are in good agreement with the modeling structure of cis-adduction (Figure 4b). There was not enough of anti-7 isolated to afford a good quality NMR spectrum. Using the empirical CD rules stated earlier, anti-6, which shows a large negative CD signal in 250–280 nm, was assigned as R and anti-7 as the S isomer.

anti-trans-BF(R,S)-N²-dG (anti-2). The MALDI mass spectrum of anti-2 showed a (M + H)⁺ ion at m/z 544 and a (M - dG)⁺ ion at m/z 428. In addition, a prominent (M + Na)⁺ peak at m/z 566 was also observed. These data suggested that anti-2 is a B[ghi]F-dG adduct. The poor solubility of this fraction in acetone is also evidence for the presence of the less lipophilic dG moiety. The overall ¹H NMR spectral pattern is analogous to anti-4, displaying well-defined connectivities among the H_{2,3,4,5,6} proton network, i.e., attachment of the exocyclic amino group of dG at C5a. The chemical shift and the $J_{3,4}$ and $J_{4,5}$ coupling constant characteristics of this fraction are very similar to those of anti-4 (Table 1), strongly suggesting that fraction 2 is formed by a trans-ring opening of the epoxide (Table 1). The CD spectrum of anti-2, however, is not as clearly defined, raising the possibility that the fraction may be a diastereomeric mixture of R and S at C5a, although repeated attempts to separate the fraction using a variety of gradient HPLC conditions were unsuccessful.

anti-trans-BF(S)-N⁷-G (anti-1). This fraction was only sparingly soluble in acetone, but very soluble in methanol. The ¹H NMR spectrum in methanol-*d*₄ showed no sugar protons. The absence of a 2'-deoxyribose was also indicated by the MALDI mass spectrum, which showed a (M + H)⁺ fragment ion of a deglycosylated adduct at m/z 428. The H_{3,4,5} methine proton connectivity was established by way of usual NOE/decoupling experiments (Table 1). It was observed that the guanine H8 proton is noticeably broad and shielded (7.25 ppm) relative to that of the corresponding dG adduct, anti-2 (8.07 ppm in acetone-*d*₆). This indicated that the guanine H8 proton is subjected to the influence of the shielding cone of the B[ghi]F aromatic moiety. Similar shielding effects of guanine H8 have been observed with N⁷-guanine adducts

derived from the diolepoxides of benzo[a]pyrene, benzo[a]anthracene, and benzo[g]chrysene (34–36). The chemical shift and coupling characteristics of anti-1 are similar to those of anti-4 and anti-5, suggesting that anti-1 is a trans-adduct. The relatively large $J_{4,5}$ coupling constant (6.6 Hz) in anti-1 may be due to the steric interaction between the deglycosylated guanine base at C5a and the pseudoaxial H4, which is supported by the calculated H5-C5C4-H4 dihedral angle (44°). The overall UV absorption pattern of anti-1 is similar to that of the deoxynucleoside adduct anti-2, but exhibited a slight hypsochromic shift (Figure 7b). The overall CD spectral pattern (Figure 8c) is similar to that of anti-5 and -7, both of which were assigned as S at C5a. Therefore, based on these data, anti-1 was identified as the deglycosylated anti-BF(S)-N⁷-Gt adduct.

anti-trans-BF(R)-N⁴-dC (anti-3). The ¹H NMR spectrum of anti-3 in acetone-*d*₆ exhibited three sets of aromatic protons in a ratio of 1:6:1. The doublet at 7.87 ppm exhibited a strong coupling and an NOE to the doublet at 5.86 ppm ($J_{5,6} = 7.5$ Hz), which is characteristic for the cytosine H5–H6 interaction (34, 37). Presence of a dC moiety was confirmed by MALDI-mass spectrum, which provided a (M + H)⁺ ion at m/z 504 and (M + H - dR)⁺ fragmentation at m/z 388. All the protons, including the B[ghi]F H_{3,4,5}-methine proton network, were assigned in the usual manner (Table 1). The overall chemical shift and coupling constant profiles of anti-3 are similar to other trans-opening adducts (i.e., anti-4, -5, -2). By analogy with anti-4 and anti-trans-tetraol, the observed $J_{3,4}$ and $J_{4,5}$ coupling constants and H5 chemical shift indicate that this dC adduct is a trans-opening adduct. The CD spectrum of anti-3 showed a strong, broad negative peak at around 280 nm (Figure 8d), a pattern similar to those of the trans-opened dC-adduct with R configuration obtained from syn-B[ghi]FDE (see following paper in this issue).

anti-trans-Tetraol and anti-cis-Tetraol. The organic phase obtained from the reaction between **2** and calf-thymus DNA (Partisil ODS2, 50% methanol in water, 1.0 mL/min) showed two peaks at 6.7 and 13.6 min in a 95:5 ratio which have been assigned to anti-trans- and anti-cis-tetraols, respectively. The MALDI mass spectra of

these two HPLC fractions give ions at m/z 301 when lithium is combined with these samples, consistent with the expected mass of the $(M + Li)^+$ ion associated with a tetraol (32). The carbinolic H3,4,5 protons in the 1H NMR spectra were assigned by analysis of decoupling, NOE, and COSY data using the general strategy described above for anti-4; the results are summarized in Table 1. As discussed above for anti-4, the incoming hydroxyl group at C5a in both tetraols must occupy the axial position. A strong upfield shift (+1.02 ppm) of H5 observed for anti-cis-tetraol relative to the trans isomer (4.80 ppm) is due to the pseudoaxial orientation of H5, which is placed under the shielding cone of the aromatic moiety. The H3–H4 dihedral angle of anti-trans-tetraol was calculated to be 145° , while that of the cis-analogue was 83° . The H4–C4–C5–H5 dihedral angle was around 60° in both cases. In accordance with this expectation, a small $J_{3,4}$ coupling constant (1.7 Hz) was observed for the minor cis-isomer at 13.6 min. A similar correlation does not exist for the major tetraol at 6.7 min, which was assigned to anti-trans-tetraol ($J_{3,4} = 7.1$ Hz, $J_{4,5} = 2.2$ Hz).

The two diastereomeric tetraols gave distinct MALDI–PSD product ion spectra when the lithium-cationized molecule ions at m/z 301 were selected for product ion analysis. A portion of this work has been published previously (32). Briefly, lithium-cationized tetraol species lose either one or two water molecules systematically, depending on the stereochemical arrangement of hydroxyl groups. For example, the $(M + Li)^+$ ion formed from anti-trans-tetraol undergoes two consecutive water eliminations to yield exclusively a single product ion at m/z 265, whereas that from the cis-tetraol loses only one mole of water to form a product ion predominantly at m/z 283. This is contrasted with the lithiated molecule ions from syn-trans-tetraol that undergo consecutive water losses to form product ions at m/z 283 and m/z 265 in equal intensities (see following paper in this issue). The syn-cis- and anti-cis tetraol gave undistinguishable PSD product ion spectra when the $(M + Li)$ ions were selected for analysis. The observed fragmentation of all four tetraols are rationalized in terms of a water loss mechanism involving a cis 1,2-elimination of trans-configuration of a vicinal hydrogen atom and hydroxyl group (32). A similar elimination reaction is not possible with a cis-diol configuration. The relative stereochemistry of hydroxyl groups at C_{3–4–5–5a} of anti-trans-, anti-cis-, syn-trans- and syn-cis-tetraols are trans-cis–trans-, trans-cis-cis-, trans-trans-trans-, and trans-trans-cis-, respectively.

UV Spectra of DNA Adducts and Tetraols. While the UV absorption spectra of each diastereomeric pair of dA adducts were virtually identical, a distinction could be made between the trans (anti-4 and -5)- and cis (anti-6 and -7)-opened dA adducts. For example, the absorption maxima of the cis-dA adducts moved toward a shorter wavelength and the shoulders are better defined than those of trans-adducts (Figure 7c). A similar trend is observed for the tetraol compounds. As compared with the tetraols, the UV spectra of dG adducts exhibited a sizable absorbance increase at 295 nm. The spectral shape for the dA and dG adducts are distinguishable. The UV spectra of the deglycosylated N⁷-substituted guanine adduct is very similar to that of the dG adducts (Figure 7b).

Discussion

We have isolated and characterized deoxynucleoside adducts and tetraols derived from the in vitro reactions of the racemic anti-B[ghi]FDE (2) with calf-thymus DNA. The structure elucidation was aided by analyses of 1H NMR, MALDI-mass, UV, and CD spectral data. Two diastereomeric pairs of dA-adducts resulting from the trans (i.e., anti-4 and -5)- or cis (i.e., anti-6 and -7)-opening of 2 have been obtained. The CD spectra of each pair are mirror images of each another (Figure 8). Tentative assignments on the absolute configuration at the site of the dA attachment were made on the basis of the empirical CD rules that have been used widely for the deoxynucleoside adducts derived from traditional diepoxides (5). A pair of trans-opening dG adducts eluted together from the reverse-phase HPLC column. No cis-opened dG adducts were isolated. Adducts formed by the trans-opening reactions with the exocyclic amino group of dC and the N⁷ of guanine have been isolated and characterized as well (Figure 3). These types of minor adducts have been previously documented (34–37). Hydrolysis of 2 gave a pair of diastereomeric trans- and cis-tetraols in a ratio of 95:5.

PSD ion MALDI mass spectra of the protonated molecular ions and source-produced BH_2^+ ions formed from the deoxynucleoside adducts were acquired to aid in adduct characterization. The fragment ion formation characteristics of the deoxynucleoside adducts are generally consistent with those of other diepoxide deoxynucleoside adducts studied previously with a variety of ionization techniques and instrumentation. However, the relative abundance of the product ions observed in the PSD spectra of the B[ghi]F-deoxynucleoside adducts differ markedly from those seen in previous product ion studies of diepoxide adducts (36, 38–41). For example, the most abundant ions observed for anti-4 are the protonated dA (m/z 252), adenine base (m/z 136), and the adenine base bound to the tri-hydroxy-B[ghi]F (m/z 412) (Figure 4). It was noted, however, that product ions formed by successive losses of H_2O and CO from B[ghi]F are much less abundant. Earlier product ion studies of protonated deoxyadenosine adducts conducted by FAB (38), ESI (36), and MALDI (39) have produced spectra that are dominated by the PAH fragments formed by successive losses of H_2O and CO. In the product ion spectra of the B[ghi]F-deoxynucleoside adducts studied here, however, the ions formed by charge retention on the PAH fragment ($R - H_2O$, m/z 259, and $R - H_2O - CO$, m/z 231) are never more than 30% relative abundance (Figure 4). The PSD spectra of the protonated BH_2^+ ions of the B[ghi]F-deoxynucleoside adducts (produced by the in-source cleavage of the glycosidic bond) are dominated by protonated nucleic acids. The PSD spectra of these protonated B[ghi]F adducts did not permit differentiation of diastereomers. The PSD spectra of the $(M + Na)^+$ molecule ions produced by deoxynucleosides adducts and tetraols provided few fragment ions and little structural information. The $(M + Li)^+$ molecule ions formed by the tetraol diastereomers, however, were found to fragment systematically by loss of one and/or two H_2O molecules depending on the relative diol stereochemistry, which greatly aided their assignments. The results are described in more detail elsewhere (32).

Normally, adducts are formed by the bonding of the benzylic carbon of PAHs to the exocyclic nitrogen of the

deoxynucleoside. The formation of these adducts may be initiated by either trans- or cis-epoxide opening. However, the structure of **2** is unique in that the two oxirane carbons are sterically crowded, one (C5a) of which is part of a completely fused ring system. Due to this sterically strained nature, however, it is possible that both C5a and C5 could be susceptible to a nucleophilic epoxide opening. It has been shown that direct aminolysis of the fjord-region anti-BcPDE (Figure 1) generates two isomeric amino alcohols in a 9:1 ratio (42). The low $\Delta\text{deloc}/\beta$ -value (43) for the benzylic C1 and the high steric congestion in the fjord-region could be contributed to the nonbenzylic opening (i.e., at C2) of the epoxide (10%). This finding, however, is contrasted with a similar reaction with the planar anti-BaPDE, which afforded only the benzylic opening product (at C10). Therefore, it was important to determine whether the oxirane ring of **2** opens in the expected manner to allow reaction with DNA bases. Although there is some evidence in the literature that the structurally similar diolepoxides derived from fluoanthene (20, 22, 44) and benzo[*b*]fluoranthene (21, 45) react with DNA in the expected manner, this needs to be demonstrated for **2**. Our ^1H NMR data provided evidence that adduct formation with **2** occurs exclusively from covalent linkage between DNA and the dibenzylic C5a, not at C5 of the epoxide. This includes an unusual deshielding of H5 and H6, the presence of the exchangeable NH proton as a singlet, and an NOE interaction between H5 and H6.

The absence of a typical benzylic proton at the site of deoxynucleoside attachment in the B[ghi]F-deoxynucleoside adducts demanded a new NMR assignment strategy. In general, H4 is recognized by its unique coupling pattern, doublet of doublets (dd), which arises from interactions with adjacent H3 and H5. The benzylic H3 is readily differentiated from H5 by the observation of its NOE and a long-range coupling to the peri aromatic proton H2, which usually resonates in the upfield aromatic region. Molecular modeling indicated that H5 in the cis-adducts, derived from anti-B[ghi]FDE, always adopts the pseudoaxial position, placing it directly under the influence of a shielding cone of the PAH ring system (Figure 6). On the other hand, the same proton in the trans-adducts adopts a pseudoequatorial position, thereby protruding away from the aromatic ring. In accordance with this, those with significant shielding of H5 (i.e., anti-6 and -7) have been assigned to the cis-adducts. It was also found that trans-adducts always exhibit a smaller $J_{4,5}$ diol coupling constant, whereas this coupling was much larger in the cis-adducts (Table 1). This is due to the fact that the incoming nucleophile (hydroxide ion or deoxynucleoside) for both trans- and cis-adducts must occupy the axial position at C5a because of the steric strain. Accordingly, the H4-C4-C5-H5 dihedral angle in the trans-adduct is close to 90° , whereas this angle is almost 0° in the cis-adduct.

In summary, we have isolated and characterized several adducts and two tetraols formed from reactions between calf-thymus DNA and **2**, a new type of structurally rigid diolepoxide. The observed adduct profiles were found to be similar to those from the extensively studied alternant PAH diolepoxides, such as BcPDE and BaPDE. This means that the reactivities at the dibenzylic C5a are comparable to the monobenzylic cationic site C1 of BcPDE and paves the way to meaningful comparative DNA-binding studies (see following paper in this issue).

Acknowledgment. We wish to thank Dr. Peter Fu for helpful discussions and Ms. Suzy Von Tungeln for her help in acquiring CD spectra.

References

- (1) Harvey, R. G. (1996) Mechanisms of carcinogenesis of polycyclic aromatic hydrocarbons. *Polycyclic Aromat. Compd.* **9**, 1–23.
- (2) Pickering, R. W. (1999) A toxicological review of polycyclic aromatic hydrocarbons. *J. Toxicol., Cutaneous Ocul. Toxicol.* **18**, 101–135.
- (3) Lichtenstein, P., Holm N. V., Verkasalo, P. K., Iliadou, A., Kaprio, J., Koskenvuo, M., Pukkala, E., Skytthe, A., and Hemminki, K. (2000) Environmental and heritable factors in the causation of cancer — analyses of cohorts of twins from Sweden, Denmark, and Finland. *N. Engl. J. Med.* **343**, 78–85.
- (4) Conney, A. H. (1982) Induction of microsomal enzymes by foreign chemicals and carcinogenesis by polycyclic aromatic hydrocarbons: G. H. A. Clowes Memorial Lecture. *Cancer Res.* **42**, 4875–4917.
- (5) Szeliga, J., and Dipple, A. (1998) DNA adduct formation by polycyclic aromatic hydrocarbon dihydrodiol epoxides. *Chem. Res. Toxicol.* **11**, 1–11.
- (6) Dipple, A., Khan, Q. A., Page, J. E., Ponten, I., and Szeliga, J. (1999) DNA reactions, mutagenic action and stealth properties of polycyclic aromatic hydrocarbon carcinogens (Review). *Intern. J. Oncol.* **14**, 103–111.
- (7) Geacintov, N. E., Cosman, M., Hingerty, B. E., Amin, S., Broyde, S., and Patel, D. J. (1997) NMR Solution structures of stereoisomeric covalent polycyclic aromatic carcinogen-DNA adducts: principles, patterns, and diversity. *Chem. Res. Toxicol.* **10**, 112–146.
- (8) Cavalieri, E. L., and Rogan, E. G. (1992) The approach to understanding aromatic hydrocarbon carcinogenesis. The central role of radical cations in metabolic activation. *Pharmacol. Ther.* **55**, 183–199.
- (9) Yang, Y., Griffiths W. J., Nordling, M., Nygren, J., Moller, L., Bergman, J., Liepinsh, E., Otting, G., Gustafsson, J. A., Rafter, J., and Sjoval, J. (2000) Ring opening of benzo[*a*]pyrene in the germ-free rat is a novel pathway for formation of potentially genotoxic metabolites. *Biochemistry* **39**, 15585–15591.
- (10) Penning, T., Burczynski, M. E., Hung, C-F., McCoull, K. D., Palackal, N. T., and Tsuruda, L. S. (1999) Dihydrodiol dehydrogenases and polycyclic aromatic hydrocarbon activation: generation of reactive and redox active o-quinones. *Chem. Res. Toxicol.* **12**, 1–18.
- (11) Buterin, T., Hess, M. T., Luneva, N., Geacintov, N. E., Amin, S., Kroth, H., Seidel, A., and Naegeli, H. (2000) Unrepaired fjord region polycyclic aromatic hydrocarbons-DNA adducts in ras codon 61 mutational hot spots. *Cancer Res.* **60**, 1849–1856.
- (12) Sundberg, K., Widersten, M., Seidel, A., Mannervik, B., and Jernstrom, B. (1997) Glutathione conjugation of bay- and fjord-region diol epoxides of polycyclic aromatic hydrocarbons by glutathione transferases M1-1 and P1-1. *Chem. Res. Toxicol.* **10**, 1221–1227.
- (13) Lin, C. H., Huang, X., Kolbanovskii, A., Hingerty, B. E., Amin, S., Broyde, S., Geacintov, N. E., and Patel, D. J. (2001) Molecular topology of polycyclic aromatic carcinogens determines DNA adduct conformation: a link to tumorigenic activity. *J. Mol. Biol.* **306**, 1059–1080.
- (14) Glatt, H., Piée, A., Pauly, K., Steinbrecher, T., Schrode, R., Oesch, F., and Seidel, A. (1991) Fjord- and bay-region diol-epoxides investigated for stability, SOS induction in *Escherichia coli*, and mutagenicity in *Salmonella typhimurium* and mammalian Cells. *Cancer Res.* **51**, 1659–1667.
- (15) Sayer, J. M., Yagi, H., Croisy-Delcey, M., and Jerina, D. M. (1981) Novel bay-region diolepoxides from benzo[*c*]phenanthrene. *J. Am. Chem. Soc.* **103**, 4970–4972.
- (16) Afshar, C. E., Katz, A. K., Carrell, H. L., Amin, S., Desai, D., and Glusker, J. (1999) Three-dimensional structure of anti-5,6-dimethylchrysene-1,2-dihydrodiol-3,4-epoxide: a diol epoxide with a bay region methyl group. *Carcinogenesis* **20**, 1549–1553.
- (17) Levin, W., Wood, A. W., Chang, R. L., Ittah, Y., Croisy-Delcey, M., Yagi, H., Jerina, D. M., and Conney, A. H. (1980) Exceptionally high tumor-initiating activity of benzo[*c*]phenanthrene bay-region diol-epoxides in mouse skin. *Cancer Res.* **40**, 3910–3914.
- (18) Agarwal, R., Canella, K. A., Yagi, H., Jerina, D. M., and Dipple, A. (1996) Benzo[*c*]phenanthrene-DNA adducts in mouse epidermis in relation to the tumorigenicities of four configurationally isomeric 3,4-dihydrodiol 1,2-epoxides. *Chem. Res. Toxicol.* **9**, 586–592.

- (19) Amin, S., Krzeminski, J., Rivenson, A., Kurtzke, C., Hecht, S. S. and El-Bayoumy, K. (1995) Mammary carcinogenicity in female CD rats of fjord region diolepoxides of benzo[c]phenanthrene, benzo[g]chrysene and dibenzo[a,l]pyrene. *Carcinogenesis* **16**, 1971–1974.
- (20) Rastetter, W. H., Nachbar, R. B., Jr., Russo-Rodriguez, S., Wattle, R. V., Thilly, W. G., Andon, B. M., Jorgensen, W. L., and Ibrahim, M. (1982) Fluoranthene: synthesis and mutagenicity of four diolepoxides. *J. Org. Chem.* **47**, 4873–4878.
- (21) He, Z.-M., Rice, J. E., and LaVoie, E. J. (1992) Synthesis of anti- and syn-diolepoxides of trans-4,5-dihydro-4,5-dihydroxybenzo[j]-fluoranthene and trans-9,10-dihydro-9,10-dihydroxy-benzo[j]fluoranthene. *J. Org. Chem.* **57**, 1784–1789.
- (22) Dai, W., Abu-Shqara, E., and Harvey, R. G. (1995) Stereoselective synthesis of putative diolepoxide metabolites of 4H-cyclopenta[def]chrysene. *J. Org. Chem.* **60**, 4905–4911.
- (23) LaVoie, E. J., He, Z.-M., Meschter, C. L., and Weyand, E. H. (1994) Tumorigenic activity of the 4,5- and 9,10-dihydrodiols of benzo[j]fluoranthene and their syn and anti diol epoxides in new born mice. *Cancer Res.* **54**, 962–968.
- (24) Amin, S., Desai, D., Dai, W., Harvey, R. G., and Hecht, S. S. (1995) Tumorigenicity in newborn mice of fjord-region and other sterically hindered diolepoxides of benzo[g]chrysene, dibenzo[a,l]pyrene (dibenzo[def,p]chrysene), 4H-cyclopenta[def]chrysene and fluoranthene. *Carcinogenesis* **16**, 2813–2817.
- (25) Wise, S. A., Benner, B. A., Byrd, G. D., Chesler, S. N., Rebbert, R. E., and Schantz, M. M. (1988) Determination of polycyclic aromatic hydrocarbons in a coal tar standard reference material. *Anal. Chem.* **60**, 887–894.
- (26) Lee, M. L., and Hites, R. A. (1976) Characterization of sulfur-containing polycyclic aromatic compounds in carbon blacks. *Anal. Chem.* **48**, 1890–1893.
- (27) Lee, M. L., and Novotny, M. (1976) Gas chromatography/mass spectrometric and nuclear magnetic resonance spectrometric studies of carcinogenic polynuclear aromatic hydrocarbons in tobacco and marijuana smoke condensates. *Anal. Chem.* **48**, 405–416.
- (28) *Survey of compounds which have been tested for carcinogenic activity* (1970–1971), PHS Publication No. 149, National Cancer Institute, NIH, PHS, 1970–1971 Volume, pp 446.
- (29) Ehrlich, H. W. W., and Beever, C. A. (1956) The crystal structure of 2:13-benzfluoranthene. *Acta Crystallogr.* **9**, 602–606.
- (30) Chang, H.-F., and Cho, B. P. (1999) Synthesis of anti- and syn-diol epoxides of trans-3,4-dihydroxy-3,4-dihydrobenzo[ghi]fluoranthene: Model planar diol epoxides. *J. Org. Chem.* **64**, 9051–9056.
- (31) Chiarelli, M. P., Gu, X., Aldridge, A. A., and Wu, H. (1998) Matrix-assisted laser desorption ionization and time-of-flight mass spectrometry for the sensitive determination of arylamide-deoxydeoxynucleoside adducts. *Anal. Chim. Acta* **368**, 1–9.
- (32) Huffer, D. M., Chang, H.-F., Cho, B. P., Zhang, L., and Chiarelli, M. P. (2001) Product ion studies of diastereomeric benzo[ghi]fluoranthene tetraols by matrix-assisted laser desorption ionization time-of-flight mass spectrometry and post-source decay. *J. Am. Soc. Mass Spectrom.* **12**, 376–380.
- (33) Wang, Y., Taylor, J.-S., and Gross, M. L. (1999) Differentiation of isomeric photomodified oligodeoxynucleotides by fragmentation of ions produced by matrix-assisted laser desorption ionization and electrospray ionization. *J. Am. Soc. Mass Spectrom.* **10**, 329–338.
- (34) Cheh, A. M., Chadha, A., Sayer, J. M., Yeh, H. J. C., Yagi, H., Pannell, L. K., and Jerina, D. M. (1993) Structures of covalent deoxynucleoside adducts formed from adenine, guanine, and cytosine bases of DNA and the optically active bay-region 3,4-diol 1,2-epoxides of benz[a]anthracene. *J. Org. Chem.* **58**, 4013–4022.
- (35) MacLeod, M. C., Evans, F. E., Lay, J., Chiarelli, P., Geacintov, N. E., Powell, K. L., Daylong, A., Luna, E., and Harvey, R. G. (1994) Identification of a novel, N7-deoxyguanosine adduct as the major DNA adduct formed by a non-bay-region diol epoxide of benzo[a]pyrene with low mutagenic potential. *Biochemistry* **33**, 2977–2987.
- (36) Szeliga, J., Page, J. E., Hilton, B. D., Kiselyov, A. S., Harvey, R. G., Dunayevskiy, Y. M., Vouros, P., and Dipple, A. (1995) Characterization of DNA adducts formed by anti-benzo[ghi]chrysene 11,12-dihydrodiol 13,14-epoxide. *Chem. Res. Toxicol.* **8**, 1014–1019.
- (37) Chadah, A., Sayer, J. M., Yeh, H. J. C., Yagi, H., Cheh, A. M., Pannell, L. K., and Jerina, D. M. (1989) Structures of covalent deoxynucleoside adducts formed from adenine, guanine, and cytosine bases in DNA and the optically active bay-region 3,4-diol 1,2-epoxides of dibenz[a,j]anthracene. *J. Am. Chem. Soc.* **111**, 5456–5463.
- (38) Li, K.-M., George, M., Gross, M. L., Seidel, A., Luch, A., Rogan, E. G., and Cavalieri, E. L. (1999) Structure elucidation of adducts formed by fjord-region dibenzo[a,l]pyrene 11,12-dihydrodiol – 13,14-epoxides and deoxyadenosine. *Chem. Res. Toxicol.* **12**, 758–767.
- (39) Stemmler, E. A., Buchanan, M. V., Hurst, G. B., and Hettich, R. L. (1994) Structural characterization of polycyclic aromatic hydrocarbon dihydrodiol epoxide adducts using matrix-assisted laser desorption/ionization Fourier transform mass spectrometry. *Anal. Chem.* **66**, 1274–1285.
- (40) Li, K.-M., George, M., Gross, M. L., Lin, C.-H., Jankowiak, R., Small, G. J., Seidel, A., Kroth, H., Rogan, E. G., and Cavalieri, E. L. (1999) Structure elucidation of adducts formed by fjord-region dibenzo[a,l]pyrene 11,12-dihydrodiol-13,14-epoxides and deoxyguanosine. *Chem. Res. Toxicol.* **8**, 778–788.
- (41) Branco, P. S., Chiarelli, M. P., Lay, J. O., Jr., and Beland, F. A. (1995) Low energy tandem mass spectrometry of deoxynucleoside adducts of polycyclic aromatic hydrocarbon dihydrodiol-epoxides. *J. Am. Soc. Mass Spectrom.* **6**, 248–256.
- (42) Lakshman, M. K., Yeh, H. J. C., Yagi, H., and Jerina, D. M. (1992) Synthesis of deoxyadenosine adducts from the highly carcinogenic fjord region-diol epoxide of benzo[c]phenanthrene. *Tetrahedron Lett.* **33**, 7121–7124.
- (43) Dewar, M. J. S. (1969) *The Molecular Orbital Theory of Organic Compounds*, McGraw-Hill, New York.
- (44) Babson, J. R., Russo-Rodriguez, S. E., Rastetter, W. H., and Wogan, G. N. (1986) *In vitro* DNA-binding of microsomally-activated fluoranthene: evidence that the major product is a fluoranthene N²-deoxyguanosine adduct. *Carcinogenesis* **7**, 859–865.
- (45) Weyand, E. H., Bryla, P., Wu, Y., He, Z.-M., and LaVoie, E. J. (1993) Detection of the major DNA adducts of benzo[j]fluoranthene in mouse skin: nonclassical dihydrodiol epoxides. *Chem. Res. Toxicol.* **6**, 117–124.

TX010133D